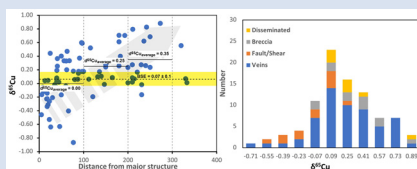# A magmatic copper and fluid source for the sediment-hosted Mount Isa deposit

I.V. Sanislav[1*], R. Mathur[2], P. Rea[3], P.H.G.M. Dirks[1],
B. Mahan[1], L. Godfrey[2], H. Degeling[4]

Abstract

OPEN ACCESS

The world class Mount Isa deposit is a unique, sediment-hosted, copper deposit with no known equivalent around the world and a controversial origin. We report $\delta^{65}Cu$ values (n = 90) from chalcopyrite grains collected systematically across the entire deposit. The $\delta^{65}Cu$ shows a unimodal distribution with limited variability (min = −0.87 ‰; max = 0.88 ‰) and an average value (+0.13 ‰) comparable to average igneous rocks. In general, the $\delta^{65}Cu$ values in chalcopyrite are lower near major structures and heavier further away, consistent with equilibrium fractionation with distance from the fluid source. The range in $\delta^{65}Cu$ of chalcopyrite from the Mount Isa deposit is less variable compared to sedimentary copper, VMS and porphyry/epithermal deposits, but similar to Michigan deposits; meanwhile, average $\delta^{65}Cu$ at Mt. Isa is distinctly higher than sedimentary copper deposits, but similar to VMS, porphyry/epithermal and Michigan deposits. These data suggest that, from a copper isotope perspective, the Mount Isa deposit is clearly different from sedimentary copper deposits and more like VMS, porphyry copper/epithermal and Michigan style deposits. The average $\delta^{65}Cu$ (+0.13 ‰) is almost identical to the average $\delta^{65}Cu$ (+0.14 ‰) from Proterozoic basalts and suggests that copper was sourced from the underlying mafic rocks; the limited fractionation and the normal distribution of the $\delta^{65}Cu$ indicate a very effective leaching mechanism and transport by a hot fluid from which chalcopyrite precipitated without significant fractionation of copper isotopes.

Introduction

The giant Mount Isa copper (with Zn-Pb) deposit, located in NW Queensland (Fig. 1), is a unique deposit type and the second largest copper producer in Australia after Olympic Dam in South Australia (*e.g.*, Mudd, 2021). Despite intense exploration for similar deposits since its discovery almost 100 years ago, Mount Isa remains the only deposit of its kind in the entire Mount Isa region and the world. Copper mineralisation occurs within the same stratigraphic horizon, the Urquhart Shales, as Zn-Pb mineralisation (Fig. 1), and the deposit is commonly described in the literature as a zoned Zn-Pb-Cu system (*e.g.*, Cave *et al.*, 2020) with copper mineralisation occurring at depth and Zn-Pb mineralisation occurring nearer the surface. Two contrasting models have been put forward to explain the source, transport and deposition of copper. The first model proposes that copper was sourced within the basin from ferruginous red beds by oxidised basinal brines and transported along permeable mud and silt horizons to the pyritic Urquhart Shales where chalcopyrite deposition occurred due to reduction reactions (*e.g.*, McGoldrick and Keays, 1990; Wilde *et al.*, 2006). The second model proposes that copper was sourced from basement mafic rocks by oxidised basinal or metamorphic brines, transported along fractures and deposited in the overlying Urquhart

Shales either by cooling, pH change or an increase in sulfur fugacity (*e.g.*, Heinrich *et al.*, 1989; Heinrich *et al.*, 1995; Gregory *et al.*, 2008). In this contribution, we present, for the first time, $^{65}Cu/^{63}Cu$ isotope data (reported as $\delta^{65}Cu$) from chalcopyrite across the Mount Isa deposit and discuss the results in terms of metal source, transport, precipitation and the two most prominent competing genetic models.

Regional and Deposit Geology

The Mount Isa Inlier (Fig. 1) has been subdivided into three sub-parallel belts that include, from east to west, the Eastern Fold Belt (EFB), the Kalkadoon-Leichardt Belt (KLB), and the Western Fold Belt (WFB). The geology of the inlier is dominated by sedimentary and volcanic sequences that were deposited in three major supra-crustal basins: 1) the 1790−1740 Ma Leichhardt Superbasin, 2) the 1730−1640 Ma Calvert Superbasin, and 3) the 1640−1580 Ma Isa Superbasin (Gibson *et al.*, 2016). These basinal sediments were deposited on top of basement rocks that had been deformed and metamorphosed during the Barramundi Orogeny (∼1890−1850 Ma; Foster and Austin, 2008). Infill of the Leichhardt Superbasin was interrupted by the ∼1750−1710 Ma Wonga Orogeny (Spence *et al.*, 2021; Spence *et al.*, 2022). Infill of

1. Economic Geology Research Centre (EGRU), James Cook University, Townsville, QLD, Australia
2. Geology Department, Juniata College, Huntingdon, PA 16652, USA
3. Mount Isa Mines, Glencore, Mount Isa, QLD, Australia
4. Geological Survey of Queensland, Brisbane, QLD, Australia
* Corresponding author (e-mail: ioan.sanislav@jcu.edu.au)
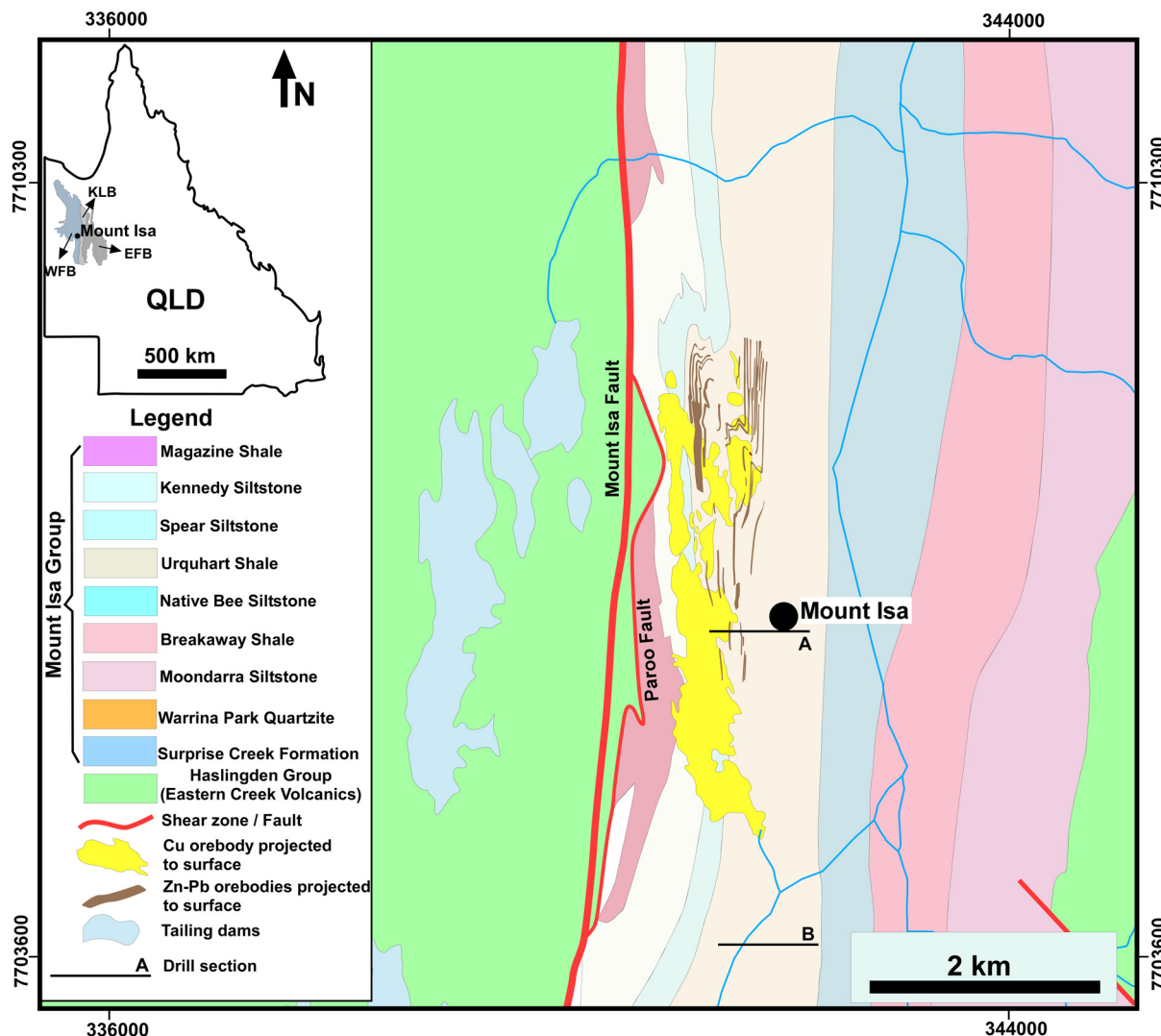
Figure 1 Simplified geological map showing the surface projection of the Cu and Zn-Pb ore bodies. The inset shows the location of the Mount Isa deposits in Queensland and within the Mount Isa Inlier. A and B indicate the location of sections shown in Figure 2. KLB-Kalkadoon Leichhardt Belt, WFB-Western Fold Belt, EFB-Eastern Fold Belt.

the Calvert Superbasin was interrupted by an inversion event between 1690 and 1668 Ma (Southgate *et al.*, 2000), and sediment fill of the Isan Superbasin was interrupted by the ~1650 −1490 Ma Isan Orogeny (Foster and Austin, 2008; Abu Sharib and Sanislav, 2013).

The Mount Isa deposit is hosted by the Mount Isa Group (Calvert Superbasin) which consists of the Surprise Creek Formation at its base, followed by the Warrina Park Quartzite, Moondara Siltstone, Breakaway Shale, Native Bee Siltstone, Urquhart Shale, Spear Siltstone, Kennedy Siltstone, and the Magazine Shale at its stratigraphic top (Southgate *et al.*, 2000). The mineralisation (Fig. 2) is hosted by the Urquhart Shales, adjacent to the Paroo Fault, which separates the Mount Isa Group from the basement mafic rocks of the Eastern Creek Volcanics (ECV). The Paroo Fault is crosscut by a series of faults (the Bernborough and J46 Faults; Fig. 2) that have been interpreted as conduits for the fluid that leached copper out of the ECV and deposited it in the Urquhart Shales (*e.g.*, Heinrich *et al.*, 1989; Heinrich *et al.*, 1995; Gregory *et al.*, 2008). The copper orebodies have irregular shapes, with highest grades in zones of most structural complexity (Fig. 2). Chalcopyrite is the dominant copper-bearing mineral; it is texturally late relative to

the Zn-Pb-Ag mineralisation (Fig. 3) and postdates peak deformation and metamorphism (*e.g.*, Cave *et al.*, 2020; Mahan *et al.*, 2023).

On a deposit scale, chalcopyrite overprints pre-existing silica-dolomite alteration. In hand specimen, the chalcopyrite occurs as infill in fracture networks that crosscut carbonaceous shale (Fig. 3a), along shear fabrics overprinting silica-dolomite alteration (Fig. 3b), replacing silica-dolomite infill of brecciated Urquhart shale (Fig. 3c) and as replacement and infill of massive silica-dolomite breccia (Fig. 3d).

Chalcopyrite δ^{65}Cu from Mount Isa Deposit

The δ^{65}Cu composition of chalcopyrite grains (Fig. 4a) were measured from ninety samples spread across the entire deposit including the surrounding low grade envelope (Supplementary Information Fig. S-2). The δ^{65}Cu values vary between −0.87 ‰ and +0.88 ‰ with an average value of +0.13 ‰ (Fig. 4a) and a median value of +0.10 ‰ which indicates that at the scale of the deposit the δ^{65}Cu values have a unimodal distribution. The
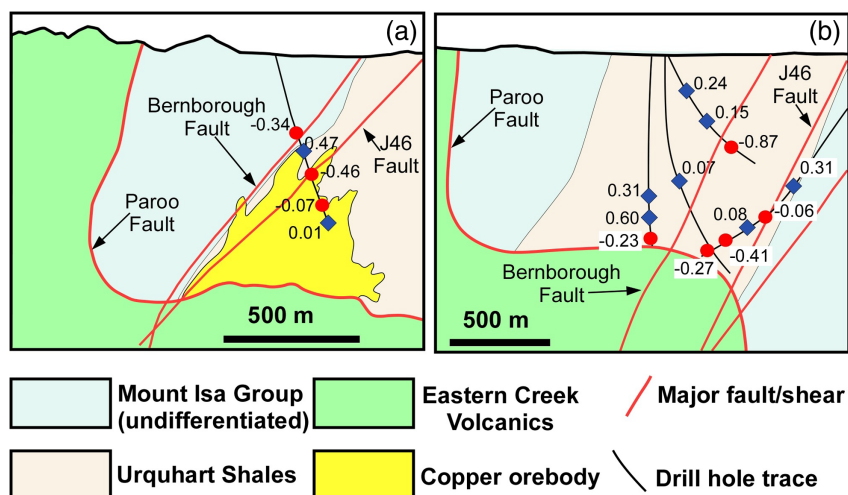
Figure 2 Cross sections through **(a)** the middle of the deposit and **(b)** across the low grade envelope showing the location of samples collected for isotope measurements and the $\delta^{65}Cu$ values for each sample. Red dots – negative values; blue diamonds – positive values.
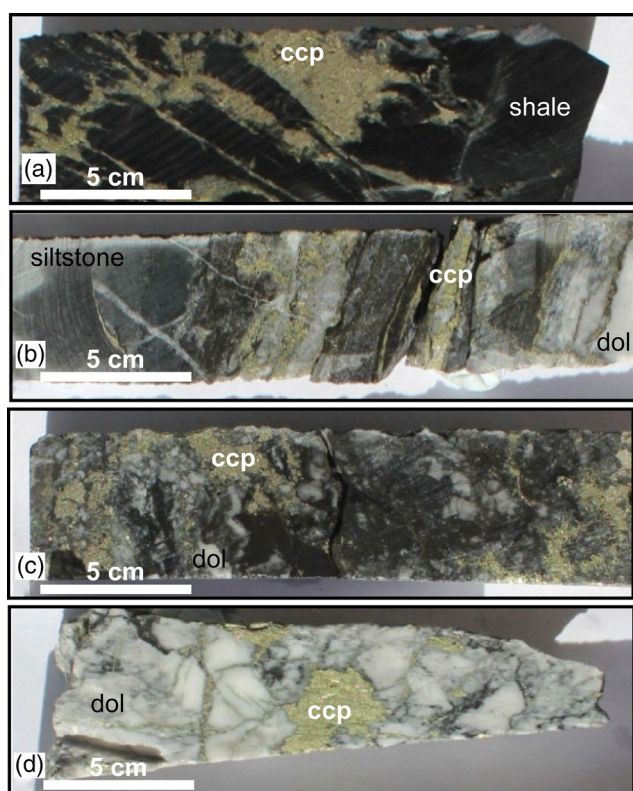
Figure 3 Photographs showing typical chalcopyrite (ccp) textures and dolomite (dol) alteration from Mount Isa deposit.
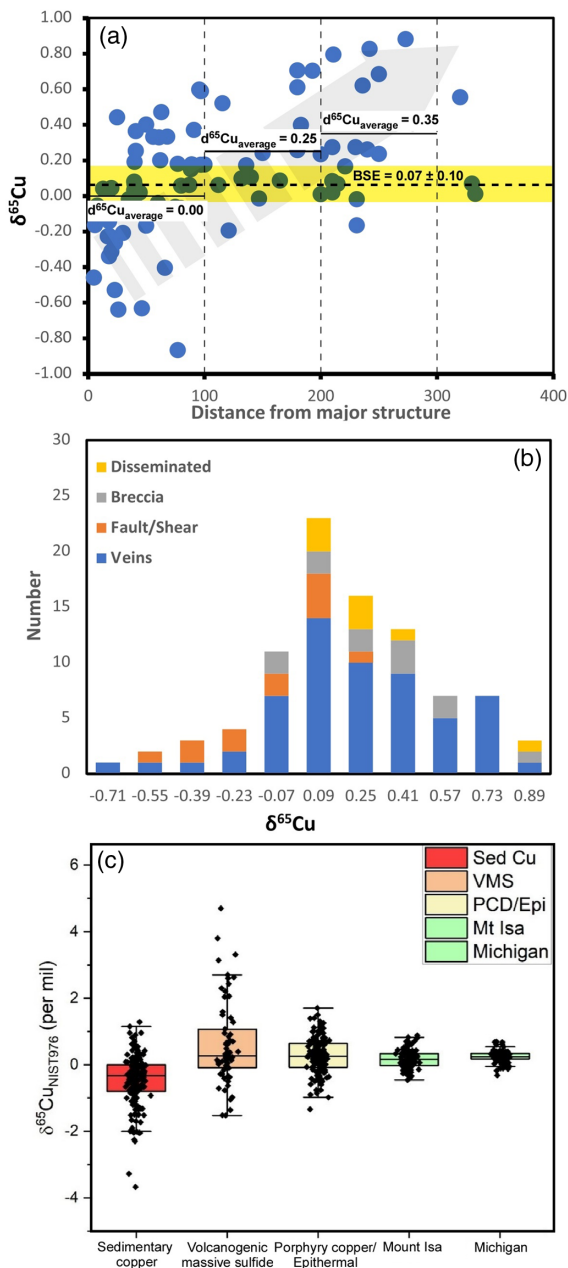
only variation in $\delta^{65}Cu$ values is in relation to the major structures. In general, lower $\delta^{65}Cu$ values occur closer to major structures whereas higher values are more common further away from these structures (Fig. 2a). Chalcopyrite grains located within 100 metres of a major structure have an average $\delta^{65}Cu = 0.00$, chalcopyrite grains located 100−200 m from a major structure have an average $\delta^{65}Cu = +0.25$ ‰ whereas chalcopyrite grains located 200−300 m have an average $\delta^{65}Cu = +0.35$ ‰ (Fig. 4a). In fact, 86 % of all negative values occur within 100 m of a major structure. The close spatial relationship between $\delta^{65}Cu$ and major structures is a general feature at the Mount Isa deposit and occurs within the deposit (Fig. 2a), more pointedly within the low grade alteration halo

(Fig. 2b) and at the scale of the entire deposit (Supplementary Information Fig. S-2). This suggests a genetic relationship between fluid pathways (major structures), the fractionation of copper isotopes and the precipitation of chalcopyrite ore. There is no clear relationship between the $\delta^{65}Cu$ values and ore textures (Fig. 4b). That is, chalcopyrite grains analysed from disseminated, breccia, fault/shear or vein-hosted ore display a similar variation in the $\delta^{65}Cu$ values.

Copper Isotopes as Indicators of Hydrothermal Fluid Pathways

The close spatial relationship (Fig. 2 and Fig. 4) between the low $\delta^{65}Cu$ values and major structures suggests that copper isotopes can be used in some cases to identify ancient hydrothermal fluid pathways with important implications for the exploration and discovery of new deposits. Lighter $\delta^{65}Cu$ values occur close to the Paroo Fault and to the steep crosscutting structures (the Bernborough and J46 Faults; Fig. 2) suggesting that these structures acted as conduits for the mineralising fluids. However, the Paroo Fault shows signs of reactivation only along the steeper sections and most likely was not an active fluid conduit during mineralisation.

The lighter $\delta^{65}Cu$ values close to the Paroo Fault can be explained by fluid ingress along the fault, at intersections with the steeper structures, and the contact with the Urquhart Shale which constitutes a strong chemical contrast. The mafic rocks of the underlying ECV constitute the most likely metal source (*e.g.,* Heinrich *et al.,* 1995; Gregory *et al.,* 2008) whereas the crosscutting steep structures such as the Bernsborough and J46 Faults represent the fluid pathways. Fluid inclusion studies, alteration and ore mineral chemistry all suggest that copper deposition at Mount Isa occurred at temperatures between 300 and 350 °C (*e.g.,* Heinrich *et al.,* 1989; Cave *et al.,* 2020). Experimental work indicates that under these conditions the $\delta^{65}Cu$ equilibrium fractionation between chalcopyrite and dissolved Cu is -0.22 ± 0.16 ‰ (Syverson *et al.,* 2021). Assuming that the ECV has an average $\delta^{65}Cu$ similar to Proterozoic basalts ($\delta^{65}Cu = +0.14$ ‰; Liu *et al.,* 2015) and that equilibrium fractionation between chalcopyrite and the hydrothermal fluid occurred, the expected $\delta^{65}Cu$ in chalcopyrite precipitated close to the fluid path (*i.e.* steep structures) will be ~ 0 ‰ whereas the $\delta^{65}Cu$ of the remaining hydrothermal fluid will have values

Figure 4 The δ^{65}Cu values for Mount Isa deposits relative to the distance from **(a)** major structures and **(b)** ore textures. **(c)** Comparison of δ^{65}Cu values from sedimentary copper deposits (Sed Cu), volcanogenic massive sulfide deposits (VMS), porphyry and epithermal deposits (PCD/Epi), Michigan copper deposits and the Mount Isa deposit.

hydrothermal systems associated with porphyry copper deposits (Gregory and Mathur, 2017). The central parts of the Pebble deposit in Alaska, the Bingham deposit in Utah, and the Grasberg deposit in Papua, Indonesia, yield copper isotope values in chalcopyrite that are lower than the distal parts of these fossilised hydrothermal systems (Gregory and Mathur, 2017; Mathur *et al.*, 2013). Similar patterns have been recognised in shallower epithermal systems in chalcopyrite and other ore minerals (Duan *et al.*, 2016; Wu *et al.*, 2017). In porphyry systems, the increase in δ^{65}Cu values away from the core of the system is related to the temperature change as the hydrothermal fluid cools down by interacting with the host rocks (Gregory and Mathur, 2017). Fluid inclusions and alteration studies (Heinrich *et al.*, 1995) at the Mount Isa deposit indicate that there is no temperature gradient away from the fluid pathways and cooling can be discarded as a major cause for isotope fractionation. Thus, the most likely cause for the observed isotope fractionation pattern is fluid reaction with the host rock. Indeed, sulfur isotope studies indicate that the sulfur required to precipitate chalcopyrite was locally derived from diagenetic pyrite within the Urquhart Shales (Heinrich *et al.*, 1995). Despite resulting from different fractionation mechanisms, the common pattern of light copper isotopes close to fluid pathways and heavier isotopes away from fluid pathways observed in porphyry copper systems and the Mount Isa deposit indicate that this could be a characteristic feature of hydrothermal systems and can be used in exploration for mineral deposits.

The Metal and Fluid Source at the Mount Isa Deposit

The main differences between the genetic models for Mount Isa deposit relate to the metal source (ferruginous red beds *vs.* basement mafic rocks), timing (syngenetic *vs.* epigenetic), and fluid source (basinal brines *vs.* metamorphic brines) (*e.g.*, Heinrich *et al.*, 1989; McGoldrick and Keays, 1990; Heinrich *et al.*, 1995; Wilde *et al.*, 2006 Gregory *et al.*, 2008; Cave *et al.*, 2020). The unimodal distribution and the low spread around the average δ^{65}Cu values measured in this study have implications for understanding the metal and the fluid source. The mafic volcanics of the ECV are significantly depleted in copper with quantitative estimates indicating at least 70 % depletion in whole rock copper from K-altered zones (*e.g.*, Heinrich *et al.*, 1995; Gregory, 2006). This suggests that copper was almost completely leached out from the sulfide and oxide phases and thus the average δ^{65}Cu most likely represents fractionation about the mean and reflects the average value of the source rock. This assumption is reasonable considering the almost identical δ^{65}Cu average (+0.13 ‰) to the average δ^{65}Cu value (+0.14 ‰) for Proterozoic basalts (Liu *et al.*, 2015) and the strong depletion in copper from the mafic volcanics surrounding the deposit. Moreover, as discussed above, the only fractionation of the copper isotopes at the scale of the deposits appears to be related to the fluid pathways and distance from major structures and is consistent with equilibrium fractionation from an evolving fluid having an average δ^{65}Cu similar to the overall deposit and typical for Proterozoic basalts. Figure 4c shows the ranges and mean δ^{65}Cu values for sedimentary copper deposits (chalcopyrite), volcanogenic massive sulfide deposits (chalcopyrite), porphyry copper (chalcopyrite and bornite) and epithermal deposits (chalcopyrite), Mount Isa (chalcopyrite) and the native copper deposits from Michigan.

Two important observations can be made. First, there is a narrow range in δ^{65}Cu for Mount Isa in comparison to all the other deposit types but the Michigan deposits. Second, the average δ^{65}Cu compositions for volcanogenic massive sulfide, porphyry copper/epithermal, Michigan and Mount Isa deposits

between 0.38−0.58 ‰ as calculated by Syverson *et al.* (2021). The average δ^{65}Cu = 0 ‰ of chalcopyrite grains collected within 100 metres (Fig. 4a) from the major structures is consistent with such calculations. Since the remaining hydrothermal fluid will be enriched in heavy isotopes, precipitation of chalcopyrite at increasing distance away from the major structures will record ever higher δ^{65}Cu values. The δ^{65}Cu$_{average}$ = 0.25 ‰ at 100−200 m and δ^{65}Cu$_{average}$ = 0.35 ‰ at 200−300 m from major structures (Figs. 2, 4a) agree with this model and indicate that equilibrium fractionation and the distance to the fluid conduits can qualitatively account for the observed variation in copper isotopes at the Mount Isa deposit.

The general increase in copper isotope values away from the fluid pathways mimics the patterns documented for

are almost identical. Although the Mount Isa deposit is sediment-hosted, its δ^{65}Cu is clearly different from sedimentary copper deposits. The sediment copper deposits form at moderate temperature compared to the other deposit types, require an oxidised source rock leached by highly oxidised basinal brines, and precipitation by mixing with a reduced fluid (*e.g.*, Hitzman *et al.*, 2010).

Copper isotopes are fractionated during oxidative alteration of clastic sediments (Mathur *et al.*, 2005; Mounyer *et al.*, 2017), and most likely the copper isotope signature of oxidised red beds is variable and departs from the average value of igneous rocks, whereas the negative fractionation seen in sedimentary copper deposits can likely be attributed to the reduction of Cu to form Cu sulfides by mixing with a reduced fluid (*e.g.*, Asael *et al.*, 2007; Asael *et al.*, 2012). The clear difference in the range and mean δ^{65}Cu signatures between sedimentary copper deposits and the Mount Isa deposit indicate that the ore forming processes (source, mobilisation and deposition) for the Mount Isa deposit are distinct from those responsible for the formation of sedimentary copper deposits, and the syn-sedimentary copper model (*e.g.*, McGoldrick and Keays, 1990; Wilde *et al.*, 2006) can be discarded.

The nearly identical average δ^{65}Cu for the Mount Isa, VMS, porphyry/epithermal and Michigan deposits overlaps with the average δ^{65}Cu for igneous rocks (BSE = +0.07 ± 0.10 ‰; Moynier *et al.*, 2017) suggesting an igneous source for copper either by leaching of igneous rocks (VMS, Michigan and Mount Isa deposits) or by separation from magma (porphyry/epithermal deposits). The wide range of δ^{65}Cu observed in VMS deposits can be explained by mixing of hot hydrothermal fluids and cold seawater during the precipitation of copper sulfides, by hydrothermal re-working of copper sulfides and by late stage low temperature processes (Rouxel *et al.*, 2004). In porphyry/epithermal deposits the large variation in δ^{65}Cu has been explained by two main processes, cooling and boiling with metal transport in a vapour phase causing significant copper and other transition metal isotope fractionation (Ikehata *et al.*, 2011; Maher *et al.*, 2011).

In the Mount Isa deposit there is no evidence that any of the processes responsible for the wide range in δ^{65}Cu values in VMS and porphyry/epithermal deposits occurred. The δ^{65}Cu values from Mount Isa deposits are almost identical to those reported from the Michigan native copper deposits suggesting a similar mineralisation process. For both deposit types, the copper was sourced from underlying mafic rocks by oxidised brines and transported upward along structures to the deposition site (*e.g.*, Bornhorst and Mathur, 2017). The almost identical average δ^{65}Cu from Mount Isa (δ^{65}Cu = 0.13 ‰) and the δ^{65}Cu measured from Proterozoic basalts (δ^{65}Cu = 0.14 ‰; Liu *et al.*, 2015) indicate that the copper was most likely sourced from the underlying ECV (Gregory *et al.*, 2008). The source of the fluid that mobilised and transported copper at Mount Isa is unlikely to be basinal or metamorphic, since the deposition of copper postdates the basin formation and metamorphism by at least 130 Myr and 60 Myr respectively (*e.g.*, Cave *et al.*, 2020). CO_2-rich fluid inclusions are subordinate, pre-date mineralisation and probably reflect peak metamorphism whereas syn-mineralisation fluid inclusions are NaCl-rich aqueous fluids with O and H isotope values overlapping the magmatic field (Heinrich *et al.*, 1989). Although, the evidence for magmatism at the time of mineralisation in the WFB is restricted to pegmatitic intrusions there is synchronous voluminous magmatism in the EFB and a magmatic source for the mineralising fluid at the Mount Isa deposit cannot be completely discarded.

Acknowledgements

Additional Information

References

Asael, D., Matthews, A., Bar-Matthews, M., and Halicz, L. (2007) Copper isotope fractionation in sedimentary copper mineralization (Timna Valley, Israel). *Chemical Geology* 243, 238–254. https://doi.org/10.1016/j.chemgeo.2007.06.007

Asael, D., Matthews, A., Bar-Matthews, M., Harlavan, Y., and Segal, I. (2012) Tracking redox controls and sources of sedimentary mineralization using copper and lead isotopes. *Chemical Geology* 310–311, 23–35. https://doi.org/10.1016/j.chemgeo.2012.03.021

Abu Sharib, A.S.A.A., and Sanislav, I.V. (2013) Polymetamorphism accompanied switching in horizontal shortening during Isan Orogeny: Example from the Eastern Fold Belt, Mount Isa Inlier, Australia. *Tectonophysics* 587, 146–167. https://doi.org/10.1016/j.tecto.2012.06.051

Bornhorst, T.J., and Mathur, R. (2017) Copper isotope constraints on the genesis of the Keweenaw Peninsula native copper district, Michigan, USA. *Minerals* 7, 185. https://doi.org/10.3390/min7100185

Cave, B., Lilly, R., and Barovich, K. (2020) Textural and geochemical analysis of chalcopyrite, galena and sphalerite across the Mount Isa Cu to Pb-Zn transition: Implications for a zoned Cu-Pb-Zn system. *Ore Geology Reviews* 124, 102647. https://doi.org/10.1016/j.oregeorev.2020.103647

Duan, J., Tang, J., Li, Y., Liu, S.-A., Wang, Q., Yang, C., and Wang, Y. (2016) Copper isotopic signature of the Tiegelongnan high-sulfidation copper deposit, Tibet: implications for its origin and mineral exploration. *Mineralium Deposita* 51, 591–602. https://doi.org/10.1007/s00126-015-0624-x

Foster, D.R.W., and Austin, J.R. (2008) The 1800–1610 Ma stratigraphic and magmatic history of the Eastern Succession, Mount Isa Inlier, and correlations with adjacent Paleoproterozoic terranes. *Precambrian Research* 163, 7–30. https://doi.org/10.1016/j.precamres.2007.08.010

Gibson, G.M., Meixner, A.J., Withnall, I.W., Korsch, R.J., Hutton, L.J., Jones, L.E.A., Holzschuh, J., Costelloe, R.D., Henson, P.A., and Saygin, E. (2016) Basin architecture and evolution in the Mount Isa mineral province, northern Australia: Constraints from deep seismic reflection profiling and implications for ore genesis. *Ore Geology Reviews* 76, 414–441. https://doi.org/10.1016/j.oregeorev.2015.07.013

Gregory, M.J. (2006) Copper mobility in the Eastern Creek Volcanics, Mount Isa, Australia: evidence from laser ablation ICP-MS of iron-titanium oxides. *Mineralium Deposita* 41, 691–711. https://doi.org/10.1007/s00126-006-0086-2

Gregory, M.J., and Mathur, R. (2017) Understanding Copper Isotope Behavior in the High Temperature Magmatic-Hydrothermal Porphyry Environment.

Geochemistry, Geophysics, Geosystems 18, 4000–4015. https://doi.org/10.1002/2017GC007026

GREGORY, M.J., KEAYS, R.R., and WILDE, A.R. (2008) Magmatic history of the Eastern Creek Volcanics, Mt Isa, Australia: insights from trace-element and platinum-group-element geochemistry. *Australian Journal of Earth Sciences* 55, 1153–1173. https://doi.org/10.1080/08120090802266618

HEINRICH, C.A., ANDREW, A.S., WILKINS, R.W.T., and PATTERSON, D.J. (1989) A fluid inclusion and stable isotope study of synmetamorphic copper ore formation at Mount Isa, Australia. *Economic Geology* 84, 529–550. https://doi.org/10.2113/gsecongeo.84.3.529

HEINRICH, C., BAIN, J.H.C., MERNAGH, T.P., WYBORN, L.A.I., ANDREW, A.S., and WARING, C.L. (1995) Fluid and mass transfer during metabasalt alteration and copper mineralization at Mount Isa, Australia. *Economic Geology* 90, 705–730. https://doi.org/10.2113/gsecongeo.90.4.705

HITZMAN, M.W., SELLEY, D., and BULL, S. (2010) Formation of Sedimentary Rock-Hosted Stratiform Copper Deposits through Earth History. *Economic Geology* 105, 627–639. https://doi.org/10.2113/gsecongeo.105.3.627

IKEHATA, K., NOTSU, K., HIRATA, T., NAVARRETE, J.U., BORROK, D.M., VIVEROS, M., and ELLZEY, J.T. (2011) Copper isotope characteristics of copper-rich minerals from Besshi-type volcanogenic massive sulfide deposits, Japan, determined using a femtosecond LA-MC-ICM-MS. *Economic Geology* 106, 307–316. https://doi.org/10.2113/econgeo.106.2.307

LIU, S.-A., HUANG, J., LIU, J., WÖRNER, G., YANG, W., TANG, Y.-J., CHEN, Y., TANG, L., ZHENG, J., and LI, S. (2015) Copper isotopic composition of the silicate Earth. *Earth and Planetary Science Letters* 427, 95–103. https://doi.org/10.1016/j.epsl.2015.06.061

MAHAN, B., MATHUR, R., SANISLAV, I., REA, P., DIRKS, P. (2023) Cu isotopes in groundwater for hydrogeochemical mineral exploration: A case study using the world-class Mount Isa Cu–Pb–Zn deposit (Australia). *Applied Geochemistry*, 148, 105519. https://doi.org/10.1016/j.apgeochem.2022.105519

MAHER, K.C., JACKSON, S., and MOUNTAIN, B. (2011) Experimental evaluation of the fluid–mineral fractionation of Cu isotopes at 250°C and 300°C. *Chemical Geology* 286, 229–239. https://doi.org/10.1016/j.chemgeo.2011.05.008

MATHUR, R., RUIZ, J., TITLEY, S., LIERMANN, L., BUSS, H., BRANTLEY, S. (2005) Cu isotopic fractionation in the supergene environment with and without bacteria. *Geochim Cosmochim Acta* 69, 5233–5246. https://doi.org/10.1016/j.gca.2005.06.022

MATHUR, R., MUNK, L., NGUYEN, M., GREGORY, M., ANNELL, H., and LANG, J. (2013) Modern and Paleofluid Pathways Revealed by Cu Isotope Compositions in Surface Waters and Ores of the Pebble Porphyry Cu-Au-Mo Deposit, Alaska. *Economic Geology* 108, 529–541. https://doi.org/10.2113/econgeo.108.3.529

McGOLDRICK, P.J., KEAYS, R.R. (1990) Mount Isa copper and lead-zinc-silver ores; coincidence or cogenesis? *Economic Geology* 85, 641–650. https://doi.org/10.2113/gsecongeo.85.3.641

MOYNIER, F., VANCE, D., FUJII, T., and SAVAGE, P. (2017) The isotope geochemistry of zinc and copper. *Reviews in Mineralogy and Geochemistry* 82, 543–600. https://doi.org/10.2138/rmg.2017.82.13

MUDD, G.M. (2021) Assessing the Availability of Global Metals and Minerals for the Sustainable Century: From Aluminium to Zirconium. *Sustainability* 13, 10855. https://doi.org/10.3390/su131910855

ROUXEL, O., FOUQUET, Y., and LUDDEN J.N. (2004) Copper isotope systematics of the Lucky Strike, Rainbow, and Logatchev Sea-Floor Hydrothermal Fields on the Mid-Atlantic Ridge. *Economic Geology* 99, 585–600. https://doi.org/10.2113/gsecongeo.99.3.585

SOUTHGATE, P.N., BRADSHAW, B.E., DOMAGALA, J., JACKSON, M.J., IDNURM, M., KRASSAY, A.A., PAGE, R.W., SAMI, T.T., SCOTT, D.L., LINDSAY, J.F., McCONACHIE, B.A., TARLOWSKI, C. (2000) Chronostratigraphic basin framework for Palaeoproterozoic rocks (1730–1575 Ma) in northern Australia and implications for base-metal mineralisation. *Australian Journal of Earth Sciences* 47, 461–483. https://doi.org/10.1046/j.1440-0952.2000.00787.x

SPENCE, J., SANISLAV, I.V., and DIRKS, P.H.G.M. (2021) 1750-1710 Ma deformation along the eastern margin of the North Australia Craton. *Precambrian Research* 353, 106019. https://doi.org/10.1016/j.precamres.2020.106019

SPENCE, J., SANISLAV, I.V., and DIRKS, P.H.G.M. (2022) Evidence for a 1750–1710 Ma orogenic event, the Wonga Orogeny, in the Mount Isa Inlier, Australia: Implications for the tectonic evolution of the North Australian Craton and Nuna Supercontinent. *Precambrian Research*, 369, 106510. https://doi.org/10.1016/j.precamres.2021.106510

SYVERSON, D.D., BORROK, D.M., NIEBUHR, S., and SEYFRIED JR, W.E. (2021) Chalcopyrite-dissolved Cu isotope exchange at hydrothermal conditions: Experimental constraints at 350°C and 50 MPa. *Geochimica et Cosmochimica Acta* 298, 191–206. https://doi.org/10.1016/j.gca.2021.02.005

WILDE, A.R., JONES, P.A., GESSNER, K., AILLERES, L., GREGORY, M.J., DUNCAN, R.J. (2006) A geochemical process model for the Mount Isa copper orebodies. *Economic Geology* 101, 1547–1567. https://doi.org/10.2113/gsecongeo.101.8.1547

WU, L.-Y., HU, R.-Z., LI, X.-F., LIU, S.-A., TANG, Y.-W., and TANG, Y.-Y. (2017) Copper isotopic compositions of the Zijinshan high-sulfidation epithermal Cu–Au deposit, South China: Implications for deposit origin. *Ore Geology Reviews*, 83, 191–199. https://doi.org/10.1016/j.oregeorev.2016.12.013

A magmatic copper and fluid source for the sediment hosted Mount Isa deposit

I.V. Sanislav, R. Mathur, P. Rea, P.H.G.M. Dirks, B. Mahan, L. Godfrey, H. Degeling

Supplementary Information

The Supplementary Information includes:

Methodology

Ninety chalcopyrite samples were collected from drill holes across well-known ore bodies and the low-grade envelope around the Mt Isa deposit. The textural position of chalcopyrite grains targeted for analysis were determined before the sulphides were analysed, and sulphides in similar textural positions were compared. Full log and assay data were available for all drill holes. The sampling strategy involved:

- to sample across the ore body from the core of the ore body to the most distal parts that contain chalcopyrite and to systematically collect samples in relationships with major structures,

- to sample within the same stratigraphic horizon,

- to sample across the entire deposit.

Chalcopyrite grains were handpicked from each sample at the Juniata College, USA and sampled with a drill dremel tool. Between 10 to 50 mg of chalcopyrite was dissolved in 4 ml of ultrapure, heated, aqua regia overnight. Due to the fact copper is a dominant ion in the mineral, no column chemistry was conducted on the chalcopyrite samples as demonstrated in (Mathur *et al.*, 2005; Zhu *et al.*, 2000; Zhang *et al.*, 2020). Isotope analyses were carried out on MC-ICP-MS instruments at various facilities (Penn State University, Washington State University and Rutgers University). Cu isotope values were corrected for mass bias using traditional standard–sample–standard bracketing with the NIST-SRM976 standard reference material and data are presented in the traditional delta notation (in per mil) compared to this standard. The instruments were in wet-plasma mode and the solutions were measured at 200 ng/g. Samples and reference materials matched to within 30 % of the ^{63}Cu signal. QA/QC for the results was monitored using an in-house USA coin (1838 USA CENT δ^{65}Cu $= 0.01 \pm 0.06$ ‰ (n=39 combined from all three locations) and BVHO-2 with values overlapping those reported in the literature.

Supplementary Tables

Table S-1 δ^{65}Cu values measured from each sample, their distance to the nearest major structure and the ore texture.

Sample ID	Section	δ^{65}Cu (‰)	Distance from major structure (meters)	Ore texture
15	MIM	-0.87	77	veins
MT03	MIM	-0.64	26	veins
30	MIM	-0.63	46.2	fault/shear
MT12	MIM	-0.53	23	fault/shear
MT11	MIM	-0.46	5	fault/shear
12	MIM	-0.41	66	veins
MT10	MIM	-0.34	18	fault/shear
8	MIM	-0.31	20	veins
38	MIM	-0.26	23.1	veins
1	MIM	-0.23	17	fault/shear
10	MIM	-0.22	18	breccia
3	MIM	-0.21	30	breccia
476	MIM	-0.20	121	veins
52	MIM	-0.17	50	fault/shear
32	MIM	-0.17	231	veins
6	MIM	-0.17	6	veins
31	MIM	-0.14	18	veins
24	MIM	-0.12	10	veins
1096	MIM	-0.12	15	veins
MT01	MIM	-0.07	80	fault/shear
11	MIM	-0.07	43	veins
9	MIM	-0.06	75	veins
36	MIM	-0.06	8	disseminated
2	MIM	-0.06	39	breccia
43	MIM	-0.04	60	veins
GF22	MIM	-0.02	35	fault/shear
479	MIM	-0.02	231	veins
11	MIM	-0.02	147	veins
28	MIM	0.01	200	veins
MT05	MIM	0.01	333	fault/shear
477	MIM	0.02	44.4	fault/shear
35	MIM	0.02	210	veins
MT07	MIM	0.03	39.6	veins
14	MIM	0.04	13	disseminated
480	MIM	0.04	20	veins
1	MIM	0.06	80	breccia
MT23-4	MIM	0.06	112	veins
26	MIM	0.06	87	veins
12	MIM	0.06	40	fault/shear
22	MIM	0.07	214.5	veins
29	MIM	0.07	330	veins
3	MIM	0.08	39.6	disseminated
478	MIM	0.08	210	veins
10	MIM	0.09	165	veins

| Sample ID	Section	$\delta^{65}Cu$ (‰)	Distance from major structure (meters)	Ore texture
7	MIM	0.10	132	veins
17	MIM	0.10	140	veins
26	MIM	0.15	88.4	veins
5	MIM	0.16	221	disseminated
39	MIM	0.17	136	disseminated
24	MIM	0.17	90	veins
4	MIM	0.17	97	disseminated
481	MIM	0.17	100	veins
40	MIM	0.18	89	breccia
15	MIM	0.18	77	veins
51	MIM	0.19	40	breccia
474	MIM	0.20	62	veins
25	MIM	0.23	200	veins
488	MIM	0.24	250	veins
14	MIM	0.24	150	veins
29	MIM	0.25	41	fault/shear
9	MIM	0.26	180	veins
8	MIM	0.26	240	breccia
487	MIM	0.27	210	veins
25	MIM	0.27	230	veins
37	MIM	0.27	150	disseminated
5	MIM	0.31	155.1	veins
23	MIM	0.33	61	veins
483	MIM	0.33	56.1	veins
7	MIM	0.33	68	veins
50	MIM	0.36	41	breccia
13	MIM	0.37	91	veins
41	MIM	0.40	183	breccia
454	MIM	0.40	50	veins
16	MIM	0.42	236	veins
27	MIM	0.43	210	veins
42	MIM	0.43	221	breccia
458	MIM	0.44	25	breccia
MT30	MIM	0.47	63	veins
MT02	MIM	0.52	115.5	veins
462	MIM	0.55	320	veins
27	MIM	0.59	97	veins
6	MIM	0.60	95.7	veins
GF23	MIM	0.61	180	veins
MT18	MIM	0.62	236	veins
451	MIM	0.68	250	veins
45	MIM	0.70	193	veins
452	MIM	0.70	180	veins
28	MIM	0.79	211	veins
2	MIM	0.83	242	breccia
MT27	MIM	0.88	273	disseminated

Supplementary Figures
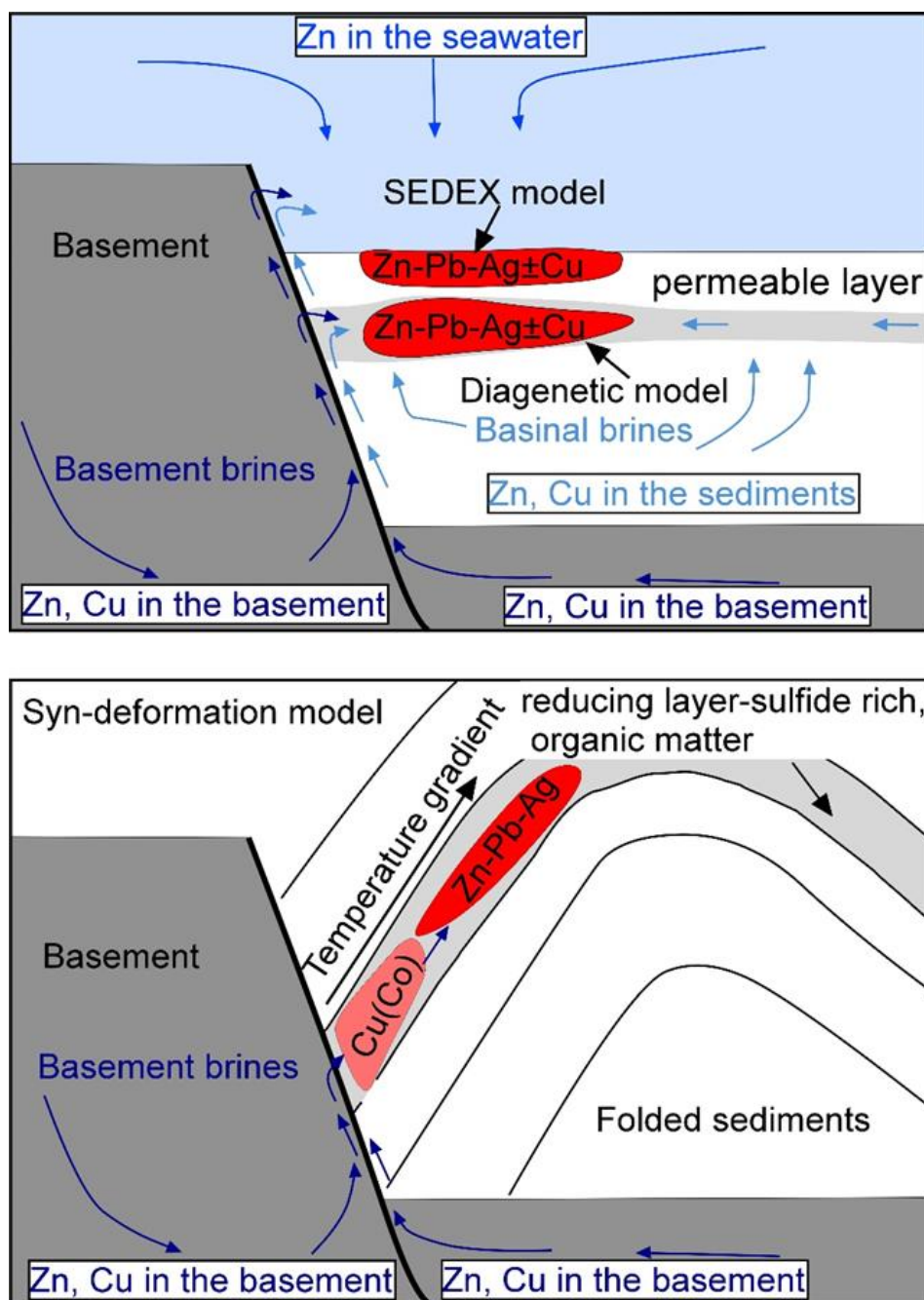
Figure S-1 Schematic representation of the two models used to explain the formation and the close spatial relationship between the Cu and Zn-Pb-Ag mineralisation at the Mount Isa deposit. The top image illustrates the syngenetic and diagenetic models whereas the bottom image illustrates the epigenetic model.
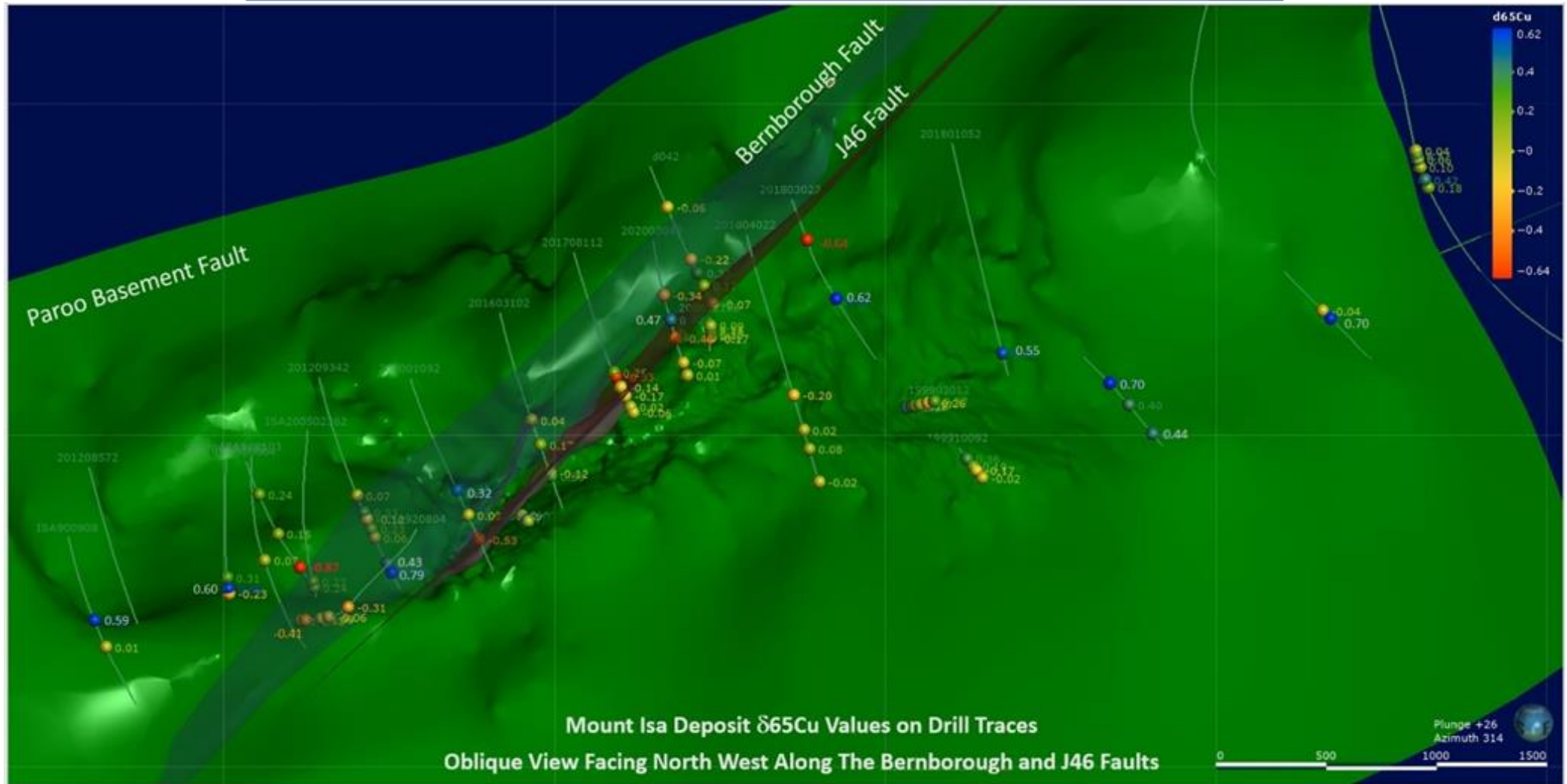
Figure S-2   Oblique view showing the distribution of samples analysed for Cu isotopes and the δ^{65}Cu values (coloured circles, corresponding to scale bar in the top right) in relationship to the main structures across the entire deposit and the surrounding low-grade envelope.
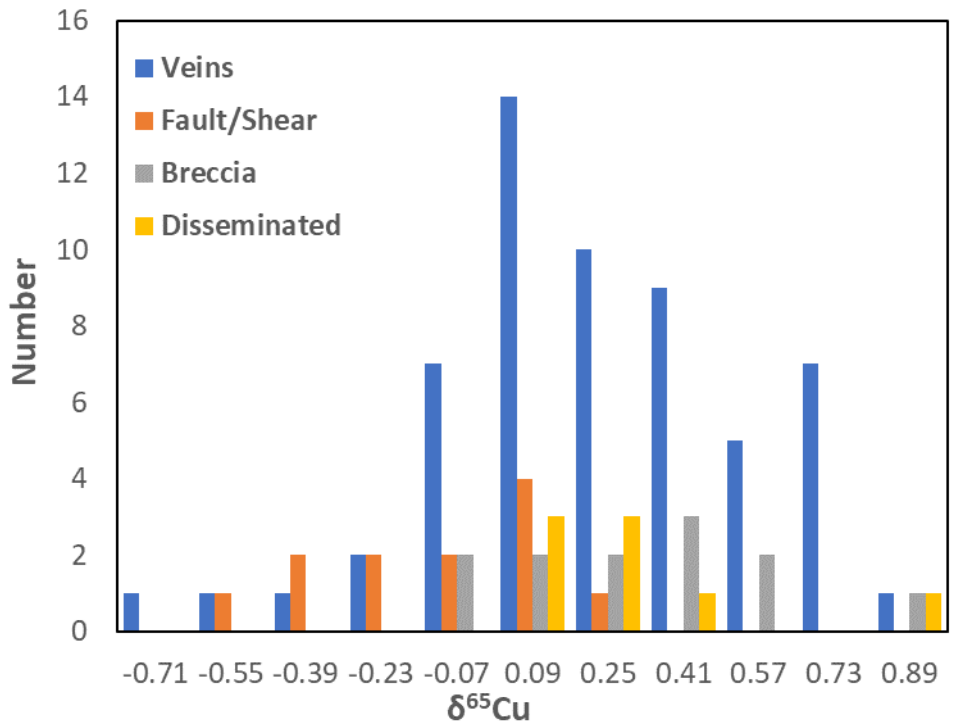
Figure S-3   Histogram showing the relationship between $\delta^{65}Cu$ and the distance to the nearest major structure.
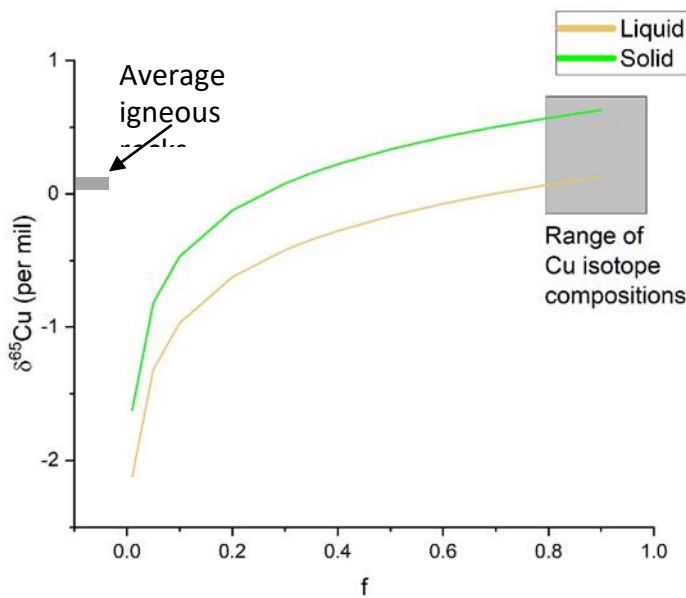
Figure S-4   Rayleigh distillation models using fractionation factors from Pekala *et al.* (2011) (alpha=1.0005) generate the observed range of fractionation measured of Mt Isa chalcopyrite for high values of f. This modelling suggests that there was an effective removal and deposition of copper in the chalcopyrite. The average $\delta^{65}Cu$ of Proterozoic basalts is +0.14‰ (Liu *et al.*, 2015) whereas the average $\delta^{65}Cu$ of the BSE is +0.07‰ (Moynier *et al.*, 2017).

Supplementary Information References

Liu, S.-A., Huang, J., Liu, J., Wörner, G., Yang, W., Tang, Y.-J., Chen, Y., Tang, L., Zheng, J., and Li, S. (2015) Copper isotopic composition of the silicate Earth. *Earth and Planetary Science Letters* 427, 95-103. https://doi.org/10.1016/j.epsl.2015.06.061

Mathur, R., Ruiz, J., Titley, S., Liermann, L., Buss, H., and Brantley, S. L. (2005) Cu isotopic fractionation in the supergene environment with and without bacteria. *Geochimica et Cosmochimica Acta* 69, 5233-5246. https://doi.org/10.1016/j.gca.2005.06.022

Moynier, F., Vance, D., Fujii, T., and Savage, P. (2017) The isotope geochemistry of zinc and copper. *Reviews in Mineralogy and Geochemistry* 82, 543-600. https://doi.org/10.2138/rmg.2017.82.13

Pekala, M., Asael, D., Butler, I. B., Matthews, A., and Rickard, D. (2011) Experimental study of Cu isotope fractionation during the reaction of aqueous Cu(II) with Fe(II) sulphides at temperatures between 40 and 2008C. *Chemical Geology* 289, 31–38. https://doi.org/10.1016/j.chemgeo.2011.07.004

Zhang, Y., Bao, Z., Lv, N., Chen, K., Zong, C., and Yuan, H. (2020) Copper isotope ratio measurements of Cu-dominated minerals without column chromatography using MC-ICP-MS. *Frontiers in Chemistry* 8, 609. https://doi.org/10.3389/fchem.2020.00609

Zhu, X. K., O'Nions, R. K., Guo, Y., Belshaw, N. S., and Rickard, D. (2000) Determination of natural Cu-isotope variation by plasma-source mass spectrometry; implications for use as geochemical tracers. *Chemical Geology* 163, 139-149. https://doi.org/10.1016/S0009-2541(99)00076-5